

Parallel Evolution of Tetrodotoxin Resistance in Three Voltage-Gated Sodium Channel Genes in the Garter Snake *Thamnophis sirtalis*

Joel W. McGlothlin,^{*1,2} John P. Chuckalovcak,^{2,3} Daniel E. Janes,^{4,5} Scott V. Edwards,⁴ Chris R. Feldman,⁶ Edmund D. Brodie Jr.,⁷ Michael E. Pfrender,⁸ and Edmund D. Brodie III^{2,9}

¹Department of Biological Sciences, Virginia Tech, Blacksburg, VA

²Department of Biology, University of Virginia

³Bio-Rad Laboratories, Hercules, CA

⁴Department of Organismic and Evolutionary Biology, Harvard University

⁵Division of Genetics and Developmental Biology, National Institutes of Health, Bethesda, MD

⁶Department of Biology, University of Nevada, Reno

⁷Department of Biology, Utah State University

⁸Department of Biological Sciences and Environmental Change Initiative, University of Notre Dame

⁹Mountain Lake Biological Station, University of Virginia

*Corresponding author: E-mail: joelmcg@vt.edu.

Associate editor: David Irwin

Abstract

Members of a gene family expressed in a single species often experience common selection pressures. Consequently, the molecular basis of complex adaptations may be expected to involve parallel evolutionary changes in multiple paralogs. Here, we use bacterial artificial chromosome library scans to investigate the evolution of the voltage-gated sodium channel (Na_v) family in the garter snake *Thamnophis sirtalis*, a predator of highly toxic *Taricha* newts. Newts possess tetrodotoxin (TTX), which blocks Na_v's, arresting action potentials in nerves and muscle. Some *Thamnophis* populations have evolved resistance to extremely high levels of TTX. Previous work has identified amino acid sites in the skeletal muscle sodium channel Na_v1.4 that confer resistance to TTX and vary across populations. We identify parallel evolution of TTX resistance in two additional Na_v paralogs, Na_v1.6 and 1.7, which are known to be expressed in the peripheral nervous system and should thus be exposed to ingested TTX. Each paralog contains at least one TTX-resistant substitution identical to a substitution previously identified in Na_v1.4. These sites are fixed across populations, suggesting that the resistant peripheral nerves antedate resistant muscle. In contrast, three sodium channels expressed solely in the central nervous system (Na_v1.1–1.3) showed no evidence of TTX resistance, consistent with protection from toxins by the blood–brain barrier. We also report the exon–intron structure of six Na_v paralogs, the first such analysis for snake genes. Our results demonstrate that the molecular basis of adaptation may be both repeatable across members of a gene family and predictable based on functional considerations.

Key words: adaptation, coevolution, gene families, molecular evolution, predator–prey interactions, toxins.

Introduction

One of the primary goals of evolutionary biology is to understand the genetic basis of adaptive phenotypic evolution. In recent years, great progress has been made toward this goal, particularly for traits that have a relatively simple genetic architecture (Rosenblum et al. 2004; Hoekstra et al. 2006; Hoekstra and Coyne 2007; Steiner et al. 2007; Stern and Orgogozo 2008), but dissecting the genetic basis of adaptation for complex polygenic phenotypes has proved somewhat elusive (Rockman 2012; Travisano and Shaw 2013). Multimember gene families, which consist of paralogs created by segmental or whole-genome duplication, are abundant across the diversity of life (Thornton and DeSalle 2000) and

provide a potential middle ground between studies of single-gene and polygenic evolution. Paralogs within gene families may have tissue-specific expression but often retain sufficiently similar functional roles. Consequently, their evolutionary response to common selection pressures may be somewhat predictable (Jost et al. 2008). If the functions of paralogs are well-characterized, then candidate genes underlying adaptation may be readily identified and investigated, providing empirical tractability similar to that of studies of single-gene evolution. At the same time, the evolution of multiple paralogs may be necessary for adaptations at the level of the whole organism. As such, studies of gene families may provide simplified models of polygenic adaptation.

Voltage-gated sodium channels (Na_v) are an excellent model system for studying both the evolution of gene families and the genetics underlying phenotypic adaptation (Liebeskind et al. 2011; Zakon 2012). These channels are formed by an α subunit consisting of four domains (DI–DIV), which together form a sodium-selective pore in the plasma membranes of excitable tissue such as nerves and muscle, and an optional β subunit that may modify its activity (Yu and Catterall 2003; Yu et al. 2005). Although invertebrate species typically have a single α subunit, vertebrates have at least four (Widmark et al. 2011; Zakon et al. 2011); these α subunits (Na_v1) are encoded by genes in the SCNA family (Catterall et al. 2005). The original expansion of the SCNA family appears to derive from the two genome duplications early in vertebrate evolution (Dehal and Boore 2005; Blomme et al. 2006), but the family has expanded further in some lineages (Widmark et al. 2011; Zakon et al. 2011). In teleost fishes, a third whole-genome duplication has expanded the family to eight members, whereas in tetrapods, duplication along chromosomes has increased the family size to six (amphibians), nine (reptiles including birds), or ten (mammals) (Zakon et al. 2011).

Na_v channels are the targets of numerous neurotoxins used as either predator venoms or prey defenses (Daly 1995; Cestèle and Catterall 2000; Fry et al. 2009). Both toxic species and their predators are expected to be under strong selection for resistance to these neurotoxins, making Na_v a model system for the evolutionary genetics of predator–prey interactions (Yoshida 1994; Geffeny et al. 2005; Jost et al. 2008; Rowe et al. 2013). One of the best characterized neurotoxins is tetrodotoxin (TTX), which acts by binding to the Na_v outer pore, which is formed by the “P-loop” region of each domain, and blocking the conductance of sodium ions across the membrane (Hanifin 2010; Moczydlowski 2013). Pufferfishes (Tetraodontidae), which employ TTX as an antipredator defense, have evolved resistance to the toxin in each of their eight Na_v paralogs through a variety of amino acid substitutions that are often shared across paralogs (Jost et al. 2008). Resistant sodium channels have also evolved in predator species that consume tetrodotoxic prey. For example, some populations of the garter snake *Thamnophis sirtalis* have evolved resistant skeletal muscle sodium channels ($\text{Na}_v1.4$) as a consequence of the ongoing coevolutionary arms race with Pacific newts (*Taricha* spp.) (Brodie and Brodie 1990; Brodie et al. 2002; Geffeny et al. 2005; Hanifin et al. 2008). Similar arms races have independently led to the convergent evolution of resistance in $\text{Na}_v1.4$ in a number of other snake species that also consume tetrodotoxic prey (Feldman et al. 2009, 2012).

Although the evolution of TTX resistance in $\text{Na}_v1.4$ has been well-characterized, little is known about how the rest of the Na_v family has evolved in *Th. sirtalis* or other predator species. In this study, we used a bacterial artificial chromosome (BAC) library and 454 sequencing to obtain the sequences of six SCNA genes from an individual *Th. sirtalis* collected from a TTX-resistant population. Three of these channels, $\text{Na}_v1.1$, $\text{Na}_v1.2$, and $\text{Na}_v1.3$ (encoded by the genes *SCN1A*, *2A*, and *3A*, respectively), are found primarily in the central nervous system (CNS) in mammals (Goldin 2001,

2002; Catterall et al. 2005). As TTX does not appear to cross the blood–brain barrier (Zimmer 2010), these channels should be sheltered from TTX, even when predatory snakes consume toxic prey. Thus, these channels should not be under selective pressure to evolve TTX resistance, and we do not expect to detect TTX resistance-conferring replacements in these loci. Three others, $\text{Na}_v1.4$, $\text{Na}_v1.6$, and $\text{Na}_v1.7$ (encoded by the genes *SCN4A*, *8A*, and *9A*), are found additionally or exclusively in the muscles or peripheral nervous system (PNS) (Caldwell et al. 2000; Thornton and DeSalle 2000; Goldin 2001, 2002; Trimmer and Rhodes 2004; Dib-Hajj et al. 2013). These tissues will be exposed to TTX when snakes consume tetrodotoxic prey, and should be under selective pressure to evolve TTX resistance. We predict that these channels will contain amino acid substitutions necessary to support TTX resistance at the organismal level and that, as in pufferfishes, TTX resistance should evolve in parallel across paralogs; that is, paralogs are expected to evolve resistance independently through similar or identical amino acid substitutions. Because our methods generated high-quality genomic sequence for most paralogs, we also report their exon–intron structure, the first such analysis for snake genes.

Results

Gene Structure

Sequences were obtained from a BAC library constructed using an individual *Th. sirtalis* from Benton County, OR, a population with medium-high resistance to TTX that coexists with the most highly tetrodotoxic population of *Taricha* newts known (Brodie et al. 2002; Hanifin et al. 2008). Complete or nearly complete genomic sequences were obtained for three paralogs: *SCN4A* (at least 65.1 kb from start codon to stop codon), *SCN8A* (73.8 kb), and *SCN9A* (56.8 kb) (fig. 1). Despite the recent publication of two snake genomes (Castoe et al. 2013; Vonk et al. 2013), to our knowledge these sodium channel genes represent the first snake genes to be presented and analyzed at the genomic sequence level. Full coding sequences (CDSs) were obtained for *SCN3A* (6,009 bp, 2,003 amino acids), *4A* (5,625 bp, 1,875 amino acids), *8A* (5,961 bp, 1,987 amino acids), and *9A* (5,892 bp, 1,964 amino acids) (supplementary table S1, Supplementary Material online). The CDS obtained for *SCN4A* was identical to the previously published sequence of the same gene from Benton County, OR, except for a single nucleotide substitution (A3427C) that led to an amino acid difference (I1143L) (Geffeny et al. 2005). Other published *SCN4A* sequences of *Th. sirtalis* from other populations have C3427/L1143 as well (Feldman et al. 2010). The CDS lengths of these four genes were comparable to their orthologs in *Rattus* and *Anolis*. Partial CDSs were obtained for *SCN1A* (5,542 bp, 1,847 amino acids) and *2A* (5,747 bp, 1,915 amino acids). Alignment of the *SCN1A* and *2A* CDS with *Rattus* and *Anolis* orthologs suggested that 483–486 bp (161–162 amino acids) and 279 bp (93 amino acids), respectively, were missing from the 3′-ends of the snake version of these genes.

The exon–intron structure of these six genes was similar to that found in other species (fig. 1). *SCN8A* and *9A* showed the

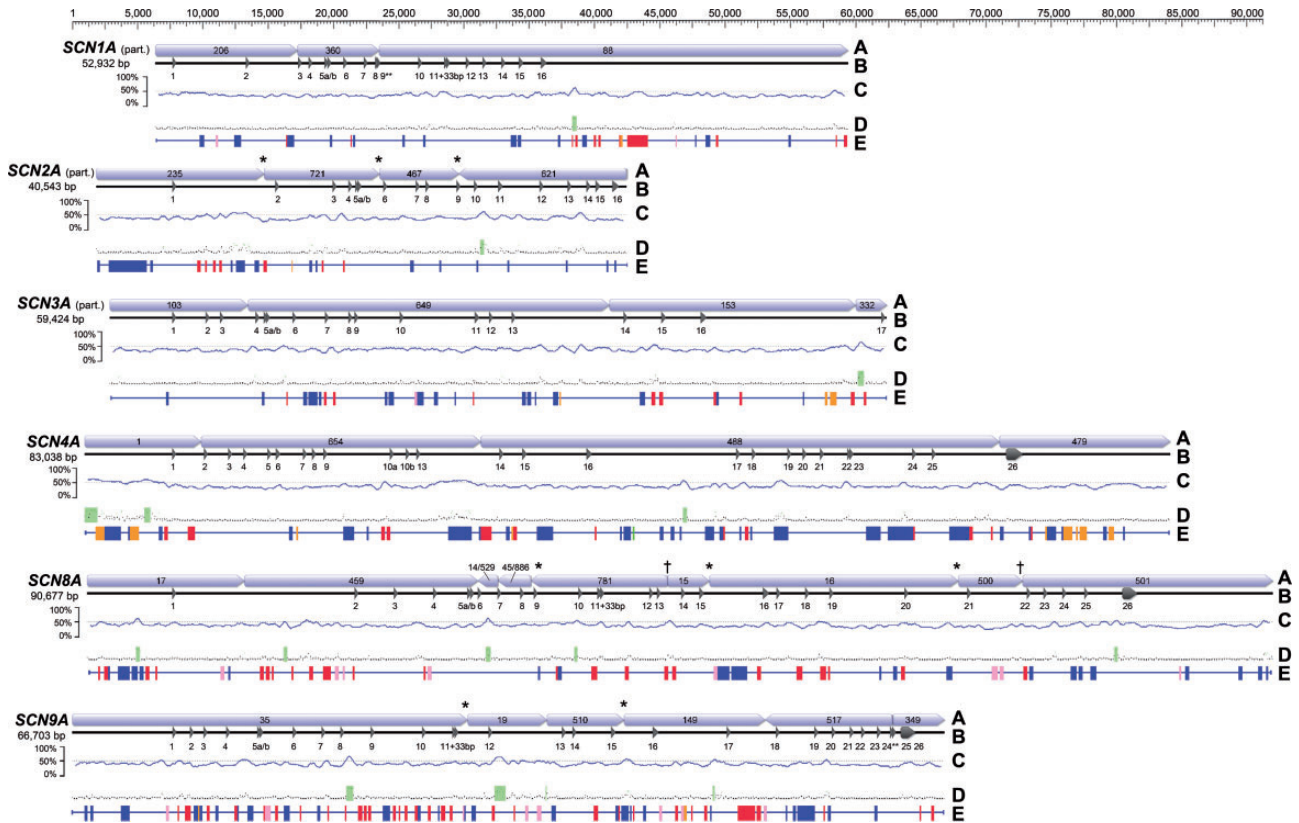


FIG. 1. Gene structure for the six *SCN4A* paralogs detected using BAC library scanning. To facilitate comparison, genes are aligned by the start codon in exon 1. Total base pair length represents the concatenated length of the contigs shown and may include untranscribed regions. (A) Concatenated contigs from 454 sequencing. (* indicates that contigs share an edge; † indicates that two contigs share an edge with a third small contig.) (B) Exon/intron structure. Partial CDS was obtained for three paralogs. (** indicates an incomplete exon.) (C) GC content using a 500-bp sliding window. (D) CpG islands (green) predicted by Geneious. (E) Simple repeats or TEs identified by Censor (green = satellite; red = DNA transposon; pink = endogenous retrovirus; orange = LTR retrotransposon; blue = non-LTR retrotransposon).

26-exon structure typical for this gene family (Widmark et al. 2011). The regions of *SCN1A*, 2A, and 3A for which we obtained genomic sequence also show typical exon–intron structure. As in most nonmammalian vertebrates, *SCN4A* has 25 exons, with two exons in place of the exons numbered 10–12 in other paralogs (Widmark et al. 2011). We have named these exons, which encode the intracellular loop linking DI and DII, 10a and 10b. Other *SCN4A* exons are numbered 1–9 and 13–26 by their homology to other paralogs following Widmark et al. (2011).

All introns with complete sequence displayed standard GT–AG ends, with exceptions in two locations. All paralogs had an AT–AC intron between exons 2 and 3 except *SCN4A*, which had an AT–AA intron in this location. There was also an AT–AC intron between exons 23 and 24 in *SCN4A*, 8A, and 9A. (We obtained only cDNA sequence for this region in the other paralogs; see Materials and Methods.) Both AT–AC introns are found in vertebrate orthologs and are thought to have an ancient origin (Widmark et al. 2011). The AT–AA intron in *SCN4A* has not been previously noted, although it is also present in *Anolis*. The lengths of completely sequenced introns ranged from 89 to 11,139 bp (median = 1,391 bp, mean = 1,837 bp). Although these lengths are typical for vertebrate genes (Hong et al. 2006),

extremely long introns may have overlapped contig boundaries, biasing the mean downward slightly. The intron between exons 16 and 17 appears to be quite long in at least four paralogs (*SCN1A*, 3A, 4A, and 9A). Although we did not detect exon 17 in *SCN1A*, contig 88 suggests that this intron may be at least 23 kb in length (fig. 1).

Putative splice variation was also present. Except for *SCN4A*, all paralogs had two copies of exon 5 separated by a short (95–147 bp) intron (fig. 1). These copies, which we call 5a and 5b, differed by 1–2 amino acids depending on the paralog. The amino acid sequence of 5b is identical across all paralogs. This exon encodes the extracellular loop between transmembrane segments S3 and S4 in domain I, and the duplication of the exon allows for alternative splicing (Copley 2004). In one paralog (*SCN5A*), this splice variation has been shown to lead to alternative neonatal and adult channels with different physiological properties (Onkal et al. 2008). Critically, this region does not seem to affect TTX sensitivity (Onkal et al. 2008). In addition, three paralogs (*SCN1A*, 8A, and 9A) have a 33-bp segment that may or may not be spliced from the end of exon 11 (fig. 1). Both types of splice variation appear to influence interaction with the β subunit (Farmer et al. 2012).

The GC content for all paralogs was approximately 40% (fig. 1), which is close to the genome-wide mean base

Table 1. Simple Repeats and TEs in SCNA Paralogs as Detected by CENSOR.

Repeat Class	SCN1A		SCN2A		SCN3A		SCN4A		SCN8A		SCN9A	
	No.	Length	No.	Length	No.	Length	No.	Length	No.	Length	No.	Length
Simple repeat	0	0	0	0	0	0	1	33	0	0	0	0
Satellite	0	0	0	0	0	0	1	33	0	0	0	0
SAT	0	0	0	0	0	0	1	33	0	0	0	0
TE	30	5,199	26	5,770	35	4,979	74	16,119	63	7,292	81	10,298
DNA transposon	11	2,277	8	948	11	986	13	1,990	29	2,213	37	4,083
Dada	0	0	1	189	0	0	1	52	0	0	0	0
Harbinger	0	0	0	0	0	0	1	119	0	0	1	39
Mariner/Tc1	5	1,811	1	73	5	473	4	1,285	12	922	17	2,545
Polinton	0	0	0	0	0	0	1	55	0	0	0	0
hAT	6	466	6	686	4	416	5	426	13	845	18	1,428
Endogenous retrovirus	2	181	0	0	1	80	0	0	9	809	9	1,118
ERV1	2	181	0	0	0	0	0	0	6	573	5	608
ERV2	0	0	0	0	0	0	0	0	2	162	3	410
ERV3	0	0	0	0	1	80	0	0	1	74	1	100
LTR retrotransposon	1	93	1	38	3	571	12	2,217	0	0	2	233
DIRS	0	0	1	38	1	102	2	153	0	0	0	0
Gypsy	1	93	0	0	2	469	9	2,020	0	0	2	233
Non-LTR retrotransposon	16	2,648	17	4,784	19	3,304	49	11,912	25	4,270	33	4,864
CR1	3	598	5	3,666	2	484	10	3,601	2	258	9	2,042
L1	3	282	2	99	0	0	8	792	1	72	3	203
L2	2	353	4	403	3	197	12	2,398	3	212	5	911
Penelope	0	0	1	208	4	808	1	117	2	163	3	231
R4	0	0	0	0	3	693	10	4,020	0	0	0	0
RTE	3	557	0	0	0	0	1	29	5	1,979	1	63
RTEX	0	0	0	0	0	0	1	127	0	0	0	0
Rex1	0	0	0	0	0	0	1	510	1	55	0	0
SINE	5	858	5	408	7	1,122	4	246	9	1,380	11	1,299
SINE2/tRNA	4	549	4	327	4	632	4	246	5	397	7	937
SINE3/5S	0	0	0	0	1	80	0	0	1	150	1	81
Tx1	0	0	0	0	0	0	1	72	1	53	0	0
Vingi	0	0	0	0	0	0	0	0	0	0	1	115
Total	30	5,199	26	5,770	34	4,979	75	16,152	63	7,292	81	10,298
% of total sequence		9.8		14.2		8.4		19.5		8.0		15.4

composition for several reptiles (Shedlock et al. 2007; Alföldi et al. 2011). However, all paralogs contained at least one CpG island, usually within introns (fig. 1). At least four paralogs (SCN1A, 3A, 4A, and 9A) had a CpG island in the long intron between exons 16 and 17. CpG islands were also detected upstream of exon 1 in two paralogs (SCN4A and 8A), suggesting a possible role in gene regulation (Deaton and Bird 2011). Transposable elements (TEs) were common in introns, making up 8–19% of noncoding regions (fig. 1, table 1). The TE profile across paralogs was comparable to that of published reptile genomes (Shedlock 2006; Alföldi et al. 2011; Castoe et al. 2013). Paralogs differed substantially in TE content (table 1). SCN4A had the highest TE content, which was primarily due to an abundance of non-LTR (long terminal repeat) retrotransposons, particularly CR1, L2, and R4, the last of which was absent from other paralogs (table 1). DNA transposons, particularly hAT and Mariner/Tc1, were most common in SCN9A, which showed the second highest TE content (table 1).

Putative TTX Resistance and Interpopulation Variation

Sodium channels expressed predominantly in the CNS ($Na_v1.1-1.3$) showed no evidence of TTX resistance evolution (fig. 2). Across all three channels, the amino acid sequence of the four P-loops was identical to the sequence from either rat or lizard. In contrast, all three channels expressed in the periphery ($Na_v1.4, 1.6,$ and 1.7) showed evidence of TTX resistance. There was no significant evidence of gene conversion between resistant paralogs, suggesting that TTX resistance initially arose through independent mutational events. However, gene conversion does appear to occur among SCN1–3/9A, which are found on the same chromosome in other amniotes (Zakon et al. 2011). Across these four paralogs, 13 CDS fragments found in seven distinct locations and averaging 120 bp in length showed evidence of gene conversion. Only one of these gene conversion events occurred in a P-loop region, the DI P-loop of SCN2/3A.

		DI	DII	DIII	DIV
Na _v 1.1/SCN1A (CNS)	<i>Rattus</i> <i>Anolis</i> <i>Thamnophis</i>	SFDTSWA <u>FLSL</u> RLMTQDFWENL	WHMNDFFHS <u>FLTIV</u> RVLGGEWIETMWDOME	NFDNVGFGYLSLLQVATFKGWMQIMYA	NFETFGNSMIGLFLQITTSAGWQGLL
Na _v 1.2/SCN2A (CNS)	<i>Rattus</i> <i>Anolis</i> <i>Thamnophis</i>	-----Y-----	---H---HH---	-----L----- -----L----- -----L-----	-----L----- -----M----- -----M-----
Na _v 1.3/SCN3A (CNS)	<i>Rattus</i> <i>Anolis</i> <i>Thamnophis</i>	-----Y----- -----Y-----	-----I-----	-----A----- -----AA----- -----A-----	-----L----- -----L----- -----L-----
Na _v 1.4/SCN4A (muscle)	<i>Rattus</i> <i>Anolis</i> <i>Thamnophis</i>	-Y-----A-----Y----- -Y-----A-----Y----- -Y-----A-----Y-----	---H---I---I---	-Y---L---L---L--- -----L----- -----L----- -----L-----	-----I---E--- -----I---M--- -----I---EV---A---
Na _v 1.6/SCN8A (PNS)	<i>Rattus</i> <i>Anolis</i> <i>Thamnophis</i>	-----A-----Y----- -----A-----Y----- -----A-----Y-----	---H---I---I---	-----A---A--- -----A---A--- -----A---A---I---	-----V----- -----V----- -----V-----
Na _v 1.7/SCN9A (PNS)	<i>Rattus</i> <i>Anolis</i> <i>Thamnophis</i>	-----A-----Y----- -----T-----Y----- -----S-----Y-----	-----Y-----	-----L----- -Y---A---A--- -----AA-----E---	-----P----- -----A----- -----A-----G---NY---

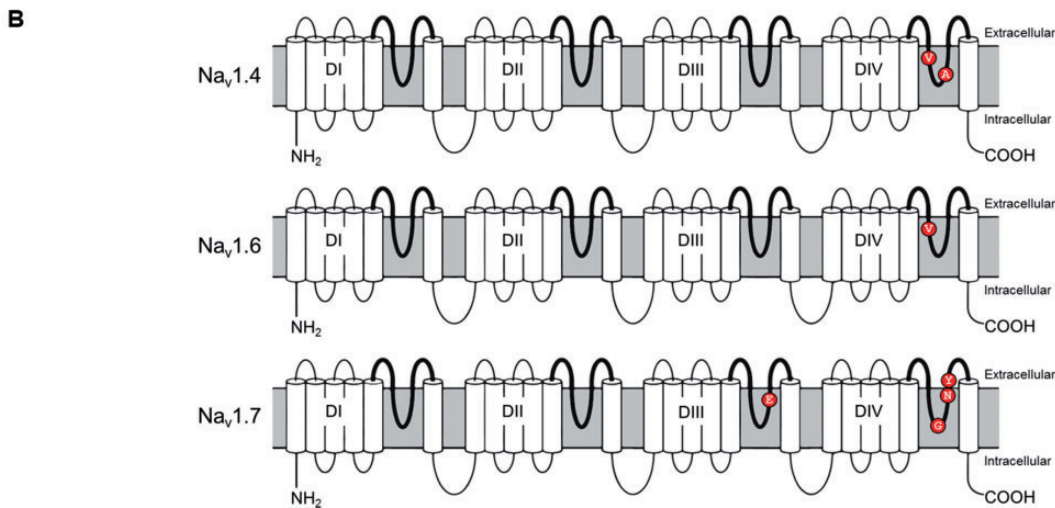


Fig. 2. (A) Amino acid substitutions in the pore regions (or “P-loops”) for six Na_v in *Thamnophis sirtalis*. All sequences are shown relative to rat Na_v1.1, with residues involved in TTX binding underlined. Substitutions putatively conferring TTX resistance are shown in red. (B) Locations of putative resistance-conferring substitutions in Na_v1.4, 1.6, and 1.7.

As previously described, the skeletal muscle channel Na_v1.4 of Benton County *Th. sirtalis* contains two substitutions in DIV: an Ile–Val (I1561V) and a Gly–Asp (G1566A). Together, these substitutions decrease the binding affinity of TTX approximately 10-fold, providing moderate TTX resistance to skeletal muscle tissue (Geffeney et al. 2002, 2005) (fig. 2).

PNS channels Na_v1.6 and 1.7 showed evidence of parallel evolution of TTX resistance. In Na_v1.6, DIV contained an Ile–Val substitution (I1709V) identical to the one seen in Na_v1.4 (fig. 2). On its own, this substitution is expected to confer 2-fold resistance to TTX (Geffeney et al. 2005). In garter snakes from Warrenton, OR, Na_v1.4 displays this Ile–Val and no other TTX-resistance substitutions, providing low to moderate levels of resistance to skeletal muscle (Geffeney et al. 2002, 2005). This finding suggests that PNS axons in *Th. sirtalis* should also display low to moderate TTX resistance.

Na_v1.7 contained four substitutions that are likely to confer resistance to TTX: An Asp–Glu (D1393E) in DIII and an Ala–Gly (A1681G), an Asp–Asn (D1684N), and a Gly–Tyr (G1685Y) in DIV (fig. 2). The Asp–Glu substitution has been previously described in Na_v1.4 from two snake species, the resistant *Th. atratus* (Feldman et al. 2009) and the putatively resistant *Amphispma pryeri* (Feldman et al. 2012), and replacements at this site lead to minor changes in TTX-binding

affinity (Terlau et al. 1991; Choudhary et al. 2003), but this specific replacement has not been empirically tested for its effects on TTX binding. The Ala–Gly substitution occurs at the channel’s selectivity filter, and is also found in four different paralogs in TTX-bearing pufferfishes, where it provides 1.5-fold resistance to TTX and 11-fold resistance to saxitoxin (Jost et al. 2008). Despite its location, this substitution does not affect ion selectivity, but delays recovery from slow inactivation (Wu et al. 2013), suggesting the possibility that it evolved to compensate for other changes to the channel’s pore. The Asp–Asn substitution occurs in a highly TTX-resistant (600X) isoform of Na_v1.4 found in California *Th. sirtalis* (Geffeney et al. 2005) and on its own should confer approximately 30- to 40-fold resistance to TTX (Penzotti et al. 1998; Choudhary et al. 2003). The Gly–Tyr substitution is previously undescribed and untested, but substitutions in this location are often found in TTX-resistant species (Geffeney et al. 2005; Jost et al. 2008; Feldman et al. 2012). This residue is located in the outer portion of the pore, and the replacement of glycine’s hydrogen with tyrosine’s large aromatic side chain may conceivably interfere with the ability of TTX to access its binding site in the pore. Taken together, these substitutions suggest that Na_v1.7 in *Th. sirtalis* should be highly resistant to TTX, protecting the function of the various tissues in which this channel is expressed (Dib-Hajj et al. 2013).

Amino acid sequences of the P-loops from Na_v1.6 DIV, and Na_v1.7 DIII and DIV obtained from 16 individual snakes from two additional populations were uniformly identical to those obtained from BAC library sequencing. These two populations differ markedly in the levels of TTX exposure individuals may experience. At Willow Creek, CA, *Th. sirtalis* coexists with *Taricha* newts of moderate toxicity (Hanifin et al. 2008) and snake resistance phenotypes are a mixture of high resistance (64%) and low resistance (36%) (Feldman et al. 2009, 2010), whereas at Mountain Lake, VA, *Notophthalmus viridescens* newts are mildly toxic (Yotsu-Yamashita and Mebs 2001) and snakes have low-resistance phenotypes (Feldman et al. 2009). Based on these P-loop sequences, all snakes were predicted to have resistant peripheral nerves regardless of their geographical origin (eastern or western North America) or their level of organismal resistance to TTX, suggesting that resistant peripheral nerves may be fixed in *Th. sirtalis*. In contrast, various alleles of Na_v1.4 associated with distinct resistance levels are found within and among populations (Geffeney et al. 2005; Feldman et al. 2009, 2010).

Incidentally, *Anolis carolinensis* Na_v1.7 also shows evidence of TTX resistance. Differences putatively conferring TTX resistance occur in two of the same sites as in *Th. sirtalis*, but with different amino acid substitutions. The Asp→Ala substitution in *A. carolinensis* DIV has previously been shown to provide approximately 150-fold resistance to TTX (Choudhary et al. 2003), and the Gly→Glu substitution adds a negative charge in the adjacent site, a feature often seen in TTX-resistant channels (Feldman et al. 2012).

Discussion

Our results indicate that the evolution of organismal resistance to ingested TTX in *Th. sirtalis* involves substitutions in at least three genes, SCN4A, SCN8A, and SCN9A, which encode three Na_v paralogs (Na_v1.4, 1.6, and 1.7, respectively) expressed in the periphery. Two peripheral nerve channels, Na_v1.6 and 1.7, show evidence of TTX-resistance evolution that parallels that previously described for skeletal muscle channel Na_v1.4 (Geffeney et al. 2005; Feldman et al. 2009, 2010). In two cases, the amino acid substitution leading to putative TTX resistance is identical across paralogs. Na_v1.7 has additional substitutions not seen in either of the other paralogs that are also expected to interfere with TTX binding. In a limited sample of individuals from across a wide geographic range (OR, CA, and VA), we found no evidence of variation in the TTX-binding region of either Na_v1.6 or Na_v1.7, suggesting either dramatically coincident replacements across populations in these genes, or more likely, that the substitutions in these two genes are fixed across the species' range. Because Na_v1.4 varies both within and among populations (Geffeney et al. 2005; Feldman et al. 2009, 2010), the latter scenario suggests that resistance in peripheral nerves is of more ancient origin than resistance in muscle. Three Na_v paralogs found primarily in the CNS, Na_v1.1–1.3, showed no evidence of TTX resistance, consistent with protection of these channels from toxins by the blood–brain barrier.

Ingested TTX has dramatic effects on peripheral nerves (Kao and Fuhrman 1963; Kiernan et al. 2005), suggesting

that both Na_v1.6 and 1.7 are likely to experience strong selection for resistance in predators that consume tetrodotoxin prey. In humans exposed to pufferfish toxin, sensory symptoms (numbness and paresthesia) occur in low-grade poisoning, with higher-grade poisoning leading to motor symptoms such as paralysis and slurred speech (Isbister and Kiernan 2005). Sensory symptoms in response to low doses of TTX likely derive from the blockade of Na_v1.7, which sets the threshold for the initiation of action potentials in sensory neurons, particularly those involved in olfaction and nociception (Dib-Hajj et al. 2013). Later motor symptoms are likely mediated by effects on Na_v1.6, which is found mainly at nodes of Ranvier, where it is involved in propagation of action potentials along axons (Caldwell et al. 2000). Human deaths from severe TTX poisoning are usually caused by respiratory failure, and evidence from laboratory mammals suggests that this effect derives from direct blockade of sodium channels in the diaphragm, which seems to be more sensitive to the toxin than most muscles (Cheng et al. 1968). However, squamates lack a diaphragm and instead power respiration with a variety of axial muscles (Rosenberg 1973; Carrier 1989). It is probable that the disruption of the motor neurons innervating this musculature contributes to respiratory failure in squamates with vulnerable Na_v1.6. Another source of mortality in TTX poisoning, especially in laboratory mammals, is severe hypotension (Zimmer 2010), which is due in part to the blockade of sympathetic nerves (Feinstein and Paimre 1968). Na_v1.7 is highly expressed in the sympathetic nervous system (Dib-Hajj et al. 2013), suggesting that TTX-induced hypotension may contribute to selection for TTX resistance in this channel.

Both western (OR, CA) and eastern (VA) populations of *Th. sirtalis* have substitutions in Na_v1.6 and 1.7 that are predicted to confer TTX resistance to peripheral nerves, but as of yet, individuals with resistant Na_v1.4 have only been detected on the west coast where the species overlaps with highly toxic *Taricha* newts (Geffeney et al. 2005). This result suggests that the origin of TTX resistance in nerves likely antedates that of TTX resistance in muscle. In general, nerves appear to be impaired by lower TTX concentrations than required to impair muscles. TTX-sensitive nerves are typically blocked by nanomolar concentrations of TTX (Kao and Fuhrman 1963), whereas blocking action potentials in muscle fibers, which tend to have diameters an order of magnitude wider than the axons that innervate them, requires concentrations an order of magnitude higher (Geffeney et al. 2002). Consequently, resistant peripheral nerves alone are likely to provide sufficient protection to allow ingestion of very small amounts of TTX, such as a garter snake might encounter when consuming the mildly toxic eastern newt *N. viridescens* (Yotsu-Yamashita and Mebs 2001). However, muscle resistance will be necessary to provide protection against the higher concentrations of TTX seen in many *Taricha* populations (Hanifin et al. 2008).

Although we suggest that resistance in Na_v1.6 and 1.7 has evolved specifically in response to selection mediated by TTX in prey, it is also possible that either or both nerve channels evolved resistance as a byproduct of selection for other functional modifications. In general, TTX-resistant substitutions

are associated with a decrease in conductance and/or sodium selectivity (Lee et al. 2011; Feldman et al. 2012). Although it is unlikely that reduced conductance or selectivity would be favored by selection in the absence of another selective agent such as TTX, other properties of sodium channels are also affected by the pore region and may be more likely targets of selection. For example, one of the substitutions in garter snake Na_v1.7 is seen in pufferfishes and a number of nontetrodotoxic fishes and has been shown to delay recovery from slow inactivation (Wu et al. 2013). Mammalian Na_v1.7 is characterized by a slow recovery from inactivation when compared with Na_v1.6 (Herzog et al. 2003), so it is possible that the Ala–Gly substitution seen in garter snakes reflects a refinement of this property. The Ile–Val substitution seen in both garter snake Na_v1.4 and Na_v1.6 has also been shown to affect slow inactivation, altering its voltage sensitivity (Lee et al. 2011). Interestingly, garter snake Na_v1.6 also has a Val–Ile substitution located in the analogous site of the DIII P-loop that may be involved in compensating for this change in voltage sensitivity.

The lack of resistance evolution in CNS channels can be attributed to the effectiveness of the blood–brain barrier against TTX. The blood–brain barrier of reptiles is similar to that of mammals (Kenny and Shivers 1974; Cserr and Bundgaard 1984) and prevents the transport of many molecules, particularly hydrophilic compounds and those of relatively high molecular weight. TTX has a molecular weight of 319.27 and is highly polar and thus lipid-insoluble. Based on these properties, one simple model (Fu et al. 2008) predicts a log ratio of steady-state brain to plasma concentrations (log BB) of -3.54 for TTX, meaning that concentrations of TTX should be 3–4 orders of magnitude lower in the brain than in the plasma. To our knowledge, there has been no direct empirical quantification of the log BB of TTX, although one early study found low concentrations of injected TTX in the brain as compared with other tissues (Kao 1966). In accordance with this observation, unconsciousness occurs only in the most severe cases of TTX poisoning in humans (Isbister and Kiernan 2005). The snake from which our BAC library was constructed coexists with the most toxic newts known (Hanifin et al. 2008), suggesting that even these newts probably do not contain enough TTX to impose selection for resistance in CNS channels. However, we predict that predator species that regularly attain higher plasma concentrations of TTX, either because they consume more toxic prey or because they have lower body weight, may evolve one or more resistant CNS channels. Highly toxic prey species, such as *Taricha*, constitutively experience high concentrations of TTX, and thus are predicted to evolve TTX resistance in all Na_v paralogs, as observed in pufferfishes (Jost et al. 2008).

We were unable to sequence Na_v1.5, 1.8, and 1.9, which are TTX resistant in mammals, using our BAC library methods. These channels were previously thought to be ancestrally resistant to TTX in vertebrates because all three paralogs share the replacement of an aromatic side chain (Tyr or Phe) with either Ser or Cys in a critical site in the DI P-loop, but recent genomic evidence has shown that these DI substitutions are not present in currently characterized teleosts,

amphibians, birds, and reptiles (Vornanen et al. 2011). Future work should examine the evolution of TTX resistance in these three channels. We predict that resistance should have evolved at least in Na_v1.5, the primary sodium channel in cardiac muscle (Goldin 2001). Despite the lack of evidence of TTX resistance of this channel in the *A. carolinensis* genome, Vornanen et al. (2011) report TTX resistance of cardiac muscle in the common European adder (*Vipera berus*), suggesting that this channel may indeed be TTX-resistant in snakes. In contrast, it is possible that organismal resistance to ingested TTX does not require resistant Na_v1.8 and 1.9. These channels are expressed in small-diameter sensory neurons and are primarily involved in nociception (Dib-Hajj et al. 2002; Fang et al. 2002; Zimmermann et al. 2007). Hypothetically, a predator with sensitive Na_v1.8 and 1.9 but resistant Na_v1.4–1.7 might experience an analgesic effect but not inhibited locomotion or respiration. At least one predator, grasshopper mice (*Onychomys* spp.), which prey upon venomous *Centruroides* scorpions, has amino acid substitutions that make the blockade of Na_v1.8 by prey toxins more likely (Rowe et al. 2013). Scorpion toxin typically causes pain by activating Na_v1.7, but in grasshopper mice, it also binds to and blocks Na_v1.8, producing a compensatory analgesic effect (Rowe et al. 2013). This blockade has no known detrimental side effects, suggesting that the blockade of Na_v1.8 with TTX may not lead to a decrease in fitness.

In summary, our results show that at least three Na_v paralogs have evolved resistance to TTX, either in garter snakes or in their ancestors. Two of the amino acid substitutions conferring resistance to TTX in the two PNS channels described here are identical to those that confer skeletal muscle resistance in the same species, and two others have been described in either other garter snakes (Feldman et al. 2009) or pufferfishes (Jost et al. 2008). Our results add to the growing consensus that evolution is often somewhat predictable at the molecular level (Stern and Orgogozo 2008, 2009). This observation seems to be particularly true for the evolution of toxin resistance in Na_v (French-Constant et al. 1998; Jost et al. 2008; Feldman et al. 2009, 2012). As in pufferfishes (Jost et al. 2008), multiple paralogs in the Na_v family have evolved resistance in parallel, but this predictability has an additional layer of complexity in garter snakes. Our results demonstrate that in predator species, TTX resistance evolves only in those channels that are routinely exposed to ingested TTX, whereas channels protected from exposure retain their sensitivity. In addition, the pattern of resistance evolution in the family suggests that channels expressed in more sensitive tissues, such as peripheral nerves, should evolve resistance prior to channels expressed in tissues whose function is impaired less severely by TTX. Future work directly testing this hypothesis will require a broader comparative approach but should reveal the ultimate origins of TTX resistance in the Na_v family.

Materials and Methods

BAC Library Scan

To obtain the genomic sequences of sodium channel genes previously uncharacterized in *Th. sirtalis*, we used radiolabeled

DNA probes to scan a BAC library, which had been previously constructed using an individual snake from Benton County, OR (<http://www.genome.gov/11008350>, last accessed April 2, 2014). This population consists of snakes with medium-high resistance to TTX and coexists with a highly toxic population of *Taricha newts* (Geffeney et al. 2005; Hanifin et al. 2008). Our approach is described only briefly below; see Janes et al. (2011) for an overview of our approach and Ross et al. (1999) for a detailed protocol.

Probes for BAC library scanning were designed using Primer3 (Koressaar and Remm 2007; Untergasser et al. 2012) and four sequence resources: The transcriptome of a related species, *Th. elegans* (Schwartz et al. 2010), the CDS of *SCN4A* from *Th. sirtalis* (Geffeney et al. 2005), the CDS of an unknown *SCNA* paralog identified using degenerate polymerase chain reaction (PCR) of brain cDNA (Chuckalovcak 2010), and the universal probe database UProbe (Kellner et al. 2005; <http://uprobe.genetics.emory.edu>, last accessed April 2, 2014). These probes fell into four categories, each of which was designed to detect one of the four major branches in the radiation of the *SCNA* family: *SCN1/2/3/9A*, *SCN4A*, *SCN5/10/11A*, and *SCN8A* (supplementary table S2, Supplementary Material online). Each probe consisted of two DNA oligomers, or “overgos” (22 or 24 bp) with 8 bp of complementary sequence at the 3′-end (supplementary table S2, Supplementary Material online). These overgos were combined in solution and radiolabeled following Ross et al. (1999), resulting in probes 36–40 bp in length.

The first 144 plates of the *Th. sirtalis* BAC library were gridded onto high-density nylon filters using a QBot gridding robot (Genetix, Ltd.) (Ross et al. 1999). Hybridization of labeled probes to these filters was performed as in Ross et al. (1999) in two steps. First, all 31 probes were pooled and 99 putative positives were identified using a Typhoon imager (GE Healthcare). Next, these putative positives were gridded onto new filters, which were hybridized with 18 smaller pools of probes to confirm positive hits (supplementary table S2, Supplementary Material online). Following this step, 31 BAC colonies were selected to be sequenced. We also added nine BAC colonies that had been previously identified using screens of the same library with *SCN4A*-specific probes (Chuckalovcak JP, unpublished data), for a total of 40 putative positives (supplementary table S3, Supplementary Material online).

DNA Isolation, Sequencing, and Assembly

These 40 colonies were cultured and BAC DNA was isolated in duplicate using a Qiagen R.E.A.L. Prep 96 Plasmid Kit. DNA concentration was quantified using a Qubit fluorometer (Invitrogen). Samples were then diluted to equal concentration (16.67 ng/μl) and pooled for sequencing. A shotgun library was prepared for 454 sequencing using standard protocols and was sequenced on two separate half-plate runs using a Roche GS-FLX with Titanium reagents at the University of Virginia (UVA) Biology Genomics Core Facility. Sequences (138 Mb) from the two half-plate runs were combined for assembly using gsAssembler 2.3 (Roche). Reads

matching the *Escherichia coli* genome or the pTarBAC2.1 vector were filtered, and default assembly settings were used. The assembly produced 812 contigs with an average size of 5,096 bp and an average read depth of 31×.

Gene Annotation

Contigs containing *SCNA* genes were initially identified with tBLASTn searches using amino acid sequences of *Th. sirtalis* Na_{1.4} (Geffeney et al. 2005) and the unknown *Th. sirtalis* paralog (Chuckalovcak 2010) as queries and the 454 output as the database. A variety of other BLAST (Basic Local Alignment Search Tool) searches using publicly available *SCNA* sequences were used to confirm these results. In all, 32 contigs ranging from 1,471 to 39,713 bp in length (average 12,416 bp) and with an average read depth of 74× were identified as containing *SCNA* exons. Most contigs contained multiple exons and the intervening intronic sequence (fig. 1). Edges between some contigs were identified by gsAssembler, providing further evidence of contig affinity (fig. 1). In two cases, two exon-containing contigs shared an edge with a third small (~20 bp) contig. Identified contigs included six versions of the first half of *SCNA* (exons 1–16), but only three versions of the second half (exons 17–26). Note that we use the numbering scheme 1–26 regardless of paralog, following Widmark et al. (2011).

To identify the specific paralog contained in each contig, we used BLAT (Kent 2002) searches against the *A. carolinensis* genome (Alföldi et al. 2011), whose paralogs were identified by Zakon et al. (2011). The results of these searches suggested that our sequences contained exons 1–16 of *SCN1A* (three contigs; exon 9 was incomplete), exons 1–16 of *SCN2A* (four contigs), exons 1–17 of *SCN3A* (four contigs), exons 1–26 of *SCN4A* (four contigs; complete CDS), exons 1–26 of *SCN8A* (11 contigs; complete CDS), and exons 1–26 of *SCN9A* (six contigs; nearly complete CDS, exon 24 was incomplete) (fig. 1). Two versions of contigs containing *SCN8A* exons 6–8 were present; these contained minor variation in intronic regions as well as a single synonymous difference in exon 8. We were unable to detect evidence of *SCN5A*, *10A*, or *11A* in our sequence. Exon–intron boundaries were identified by comparing sequences to published genomes (*A. carolinensis* and *Homo sapiens*). The exon–intron structure of contigs was annotated using Geneious 6.1.7 (Biomatters). We also used algorithms within Geneious 6.1.7 to measure GC content and to detect CpG islands. To explore the genomic content of intronic sequence, contigs were screened against a database of vertebrate simple repeats and TEs (Repbase) using Censor (Kohany et al. 2006).

Gap Filling

Gaps in the CDS for *SCN1A*, *2A*, and *3A* were filled using Sanger sequencing of brain cDNA, which was obtained from a captive adult female *Th. sirtalis* that had been previously captured from the highly TTX-resistant population in Willow Creek, CA. The CDSs for exons 14–26 of *SCN1A* (44 reads, 3,114 bp, 4.7× coverage, 92% of sequence from both strands), exons 16–26 of *SCN2A* (32 reads, 2,632 bp, 4.3×, 77%

from both strands), and exons 17–26 of *SCN3A* (38 reads, 2,821 bp, 4.4×, 79% from both strands) were obtained using primers designed from the transcriptome of *Th. elegans* (Schwartz et al. 2010) (supplementary table S5, Supplementary Material online). We attempted 3′-RACE (Rapid Amplification of cDNA Ends) to obtain the sequences of the 3′-ends of transcripts, but this gave low-quality sequence in *SCN1A* and was unsuccessful in *SCN2A*; therefore, the sequences of exon 26 were incomplete for these paralogs (690 and 916 bp, respectively). The complete CDS of exon 26 (1,193 bp, including the stop codon) plus 222 bp 3′-UTR was obtained for *SCN3A*. The CDS for the missing segment of *SCN1A* exon 9 was obtained using primers designed from contigs 360 and 88 of our 454 run (supplementary table S5, Supplementary Material online). Finally, CDS for the missing segment of *SCN9A* exon 24 was obtained from previous degenerate PCR results (Chuckalovcak 2010), as BLAST searches against our 454 contigs showed that sequence containing exons 19–26 obtained through this method belonged to *SCN9A*. All PCR followed standard protocols, and post-PCR cleanup was achieved using a combination of exonuclease I and shrimp alkaline phosphatase (Exo-SAP, USB). Sequencing was carried out either on an ABI 3130 at UVA's Genomics Core Facility or on an ABI 3730 at Yale University's DNA Analysis Facility.

Paralog Identification

The identity of each paralog was confirmed by using BLAT searches of the entire CDS against the *A. carolinensis* genome. The best BLAT hit was invariably the paralog assigned using our preliminary BLAT searches of separate contigs (supplementary table S4, Supplementary Material online). We also constructed a protein phylogeny of the six *Th. sirtalis* paralogs and all nine *A. carolinensis* paralogs (Zakon et al. 2011, accession nos. BK007953–BK007961). Amino acid sequences were aligned using MUSCLE (Edgar 2004) and a maximum-likelihood phylogeny was constructed using PhyML (Guindon and Gascuel 2003). Each *Th. sirtalis* paralog was shown to be most similar to its assigned ortholog in *A. carolinensis*, and each of these nodes had a bootstrap value of 100 (supplementary fig. S1, Supplementary Material online). We tested for evidence of gene conversion among paralogs using a MUSCLE alignment of the six *Th. sirtalis* paralogs in GENECONV (Sawyer 1989).

Putative TTX Resistance and Interpopulation Variation

We scanned for putative TTX resistance by comparing the P-loop regions from CDS of the six paralogs we identified to reference sequence from both *A. carolinensis* and a mammal (the rat *Rattus norvegicus*). From paralogs whose sequences indicated putative TTX resistance, we also examined sequences from individuals from two populations: Willow Creek, CA, which consists of a mixture of low- and high-resistance individuals (Feldman et al. 2009, 2010) and Mountain Lake Biological Station, VA, which displays low resistance and occurs outside the range of *Taricha* but overlaps with the mildly toxic *N. viridescens* (Yotsu-Yamashita and Mebs 2001).

We used tissue samples from 16 individual snakes whose *SCN4A* genotypes and organismal resistance were reported by Feldman et al. (2009): CA high-resistance $n = 10$ (*SCN4A* accession nos. FJ571047–FJ571056), CA low-resistance $n = 1$ (GQ154075), and VA $n = 4$ (FJ571057–FJ571060). Sample sizes for individual regions were as follows: *SCN8A* DIII and DIV, CA high-resistance $n = 2$, VA $n = 2$; *SCN9A* DIII CA high-resistance $n = 10$, CA low-resistance $n = 1$, VA $n = 1$; *SCN9A* DIV CA high-resistance $n = 10$, CA low-resistance $n = 1$, VA $n = 4$. Primers were designed from our 454 contigs (supplementary table S6, Supplementary Material online). PCR and cleanup were carried out as above, and sequencing was performed on an ABI 3730 at the Yale DNA Analysis Facility.

Accession Numbers

All new sequences have been deposited in GenBank under accession numbers KJ908861–KJ908938 and KM066119. The predicted CDSs for each paralog have been deposited as Third Party Annotations under accession numbers BK008860–BK008865.

Supplementary Material

Supplementary figure S1 and tables S1–S6 are available at *Molecular Biology and Evolution* online (<http://www.mbe.oxfordjournals.org/>).

Acknowledgments

The authors thank Michelle Sivilich and Megan Kobiela for assistance in the laboratory, Dan Sloan for advice on molecular techniques, Shana Geffeny and Charles Hanifin for helpful discussions, Nigel Delaney and Yoel Stuart for logistical support in Cambridge, and Angela Hornsby, Marjorie Matocq, and Kendra Sewall for comments on the manuscript. This material is based upon work supported by the National Science Foundation (grant numbers DEB 0922216 to E.D.B. III and DEB 1034686 to M.E.P.). Publication of this article was supported by Virginia Tech's Open Access Subvention Fund.

References

- Alföldi J, Di Palma F, Grabherr M, Williams C, Kong LS, Mauceli E, Russell P, Lowe CB, Glor RE, Jaffe JD, et al. 2011. The genome of the green anole lizard and a comparative analysis with birds and mammals. *Nature* 477(7366):587–591.
- Blomme T, Vandepoel K, De Bodt S, Simillion C, Maere S, Van de Peer Y. 2006. The gain and loss of genes during 600 million years of vertebrate evolution. *Genome Biol.* 7(5):R43.
- Brodie ED III, Brodie ED Jr. 1990. Tetrodotoxin resistance in garter snakes: an evolutionary response of predators to dangerous prey. *Evolution* 44(3):651–659.
- Brodie ED Jr, Ridenhour BJ, Brodie ED III. 2002. The evolutionary response of predators to dangerous prey: hotspots and coldspots in the geographic mosaic of coevolution between garter snakes and newts. *Evolution* 56(10):2067–2082.
- Caldwell JH, Schaller KL, Lasher RS, Peles E, Levinson SR. 2000. Sodium channel Na_v1.6 is localized at nodes of Ranvier, dendrites, and synapses. *Proc Natl Acad Sci U S A.* 97(10):5616–5620.
- Carrier DR. 1989. Ventilatory action of the hypaxial muscles of the lizard *Iguana iguana*: a function of slow muscle. *J Exp Biol.* 143:435–457.
- Castoe TA, de Koning APJ, Hall KT, Card DC, Schield DR, Fujita MK, Ruggiero RP, Degner JF, Daza JM, Gu WJ, et al. 2013. The Burmese

- python genome reveals the molecular basis for extreme adaptation in snakes. *Proc Natl Acad Sci U S A*. 110(51):20645–20650.
- Catterall WA, Goldin AL, Waxman SG. 2005. International Union of Pharmacology. XLVII. Nomenclature and structure-function relationships of voltage-gated sodium channels. *Pharmacol Rev*. 57(4):397–409.
- Cestèle S, Catterall WA. 2000. Molecular mechanisms of neurotoxin action on voltage-gated sodium channels. *Biochimie* 82(9–10):883–892.
- Cheng K, Ling Y, Wang JC. 1968. The failure of respiration in death by tetrodotoxin poisoning. *Q J Exp Physiol*. 53:119–128.
- Choudhary G, Yotsu-Yamashita M, Shang L, Yasumoto T, Dudley SC. 2003. Interactions of the C-11 hydroxyl of tetrodotoxin with the sodium channel outer vestibule. *Biophys J*. 84(1):287–294.
- Chuckalovcak JP. 2010. Identification and characterization of a novel voltage-gated sodium channel gene in the tetrodotoxin resistant garter snake *Thamnophis sirtalis* [master's thesis]. Charlottesville (VA): University of Virginia.
- Copley RR. 2004. Evolutionary convergence of alternative splicing in ion channels. *Trends Genet*. 20(4):171–176.
- Cserr HF, Bundgaard M. 1984. Blood-brain interfaces in vertebrates: a comparative approach. *Am J Physiol*. 246(3):R277–R288.
- Daly JW. 1995. The chemistry of poisons in amphibian skin. *Proc Natl Acad Sci U S A*. 92(1):9–13.
- Deaton AM, Bird A. 2011. CpG islands and the regulation of transcription. *Gene Dev*. 25(10):1010–1022.
- Dehal P, Boore JL. 2005. Two rounds of whole genome duplication in the ancestral vertebrate. *PLoS Biol*. 3(10):1700–1708.
- Dib-Hajj S, Black JA, Cummins TR, Waxman SG. 2002. Na_v/Na_v1.9: a sodium channel with unique properties. *Trends Neurosci*. 25(5):253–259.
- Dib-Hajj SD, Yang Y, Black JA, Waxman SG. 2013. The Na_v1.7 sodium channel: from molecule to man. *Nat Rev Neurosci*. 14(1):49–62.
- Edgar RC. 2004. MUSCLE: multiple sequence alignment with high accuracy and high throughput. *Nucleic Acids Res*. 32(5):1792–1797.
- Fang X, Djouhri L, Black JA, Dib-Hajj SD, Waxman SG, Lawson SN. 2002. The presence and role of the tetrodotoxin-resistant sodium channel Na_v1.9 (NaN) in nociceptive primary afferent neurons. *J Neurosci*. 22(17):7425–7433.
- Farmer C, Cox JJ, Fletcher EV, Woods CG, Wood JN, Schorge S. 2012. Splice variants of Nav1.7 sodium channels have distinct β subunit-dependent biophysical properties. *PLoS One* 7(7):e41750.
- Feinstein MB, Paimre M. 1968. Mechanism of cardiovascular action of tetrodotoxin in the cat. Block of conduction in peripheral sympathetic fibers. *Circ Res*. 23(4):553–565.
- Feldman CR, Brodie ED Jr, Brodie ED III, Pfrender ME. 2009. The evolutionary origins of beneficial alleles during the repeated adaptation of garter snakes to deadly prey. *Proc Natl Acad Sci U S A*. 106(32):13415–13420.
- Feldman CR, Brodie ED Jr, Brodie ED III, Pfrender ME. 2010. Genetic architecture of a feeding adaptation: garter snake (*Thamnophis*) resistance to tetrodotoxin bearing prey. *Proc R Soc Lond B Biol Sci*. 277(1698):3317–3325.
- Feldman CR, Brodie ED Jr, Brodie ED III, Pfrender ME. 2012. Constraint shapes convergence in tetrodotoxin-resistant sodium channels of snakes. *Proc Natl Acad Sci U S A*. 109(12):4556–4561.
- French-Constant RH, Pittendrigh B, Vaughan A, Anthony N. 1998. Why are there so few resistance-associated mutations in insecticide target genes? *Philos Trans R Soc Lond B* 353(1376):1685–1693.
- Fry BG, Roelants K, Champagne DE, Scheib H, Tyndall JDA, King GF, Nevalainen TJ, Norman JA, Lewis RJ, Norton RS, et al. 2009. The toxicogenomic multiverse: convergent recruitment of proteins into animal venoms. *Annu Rev Genomics Hum Genet*. 10:483–511.
- Fu XC, Wang GP, Shan HL, Liang WQ, Gao JQ. 2008. Predicting blood-brain barrier penetration from molecular weight and number of polar atoms. *Eur J Pharm Biopharm*. 70(2):462–466.
- Geffeney S, Brodie ED Jr, Ruben PC, Brodie ED III. 2002. Mechanisms of adaptation in a predator-prey arms race: TTX-resistant sodium channels. *Science* 297(5585):1336–1339.
- Geffeney SL, Fujimoto E, Brodie ED III, Brodie ED Jr, Ruben PC. 2005. Evolutionary diversification of TTX-resistant sodium channels in a predator-prey interaction. *Nature* 434(7034):759–763.
- Goldin AL. 2001. Resurgence of sodium channel research. *Annu Rev Phys*. 63:871–894.
- Goldin AL. 2002. Evolution of voltage-gated Na⁺ channels. *J Exp Biol*. 205(5):575–584.
- Guindon S, Gascuel O. 2003. A simple, fast, and accurate algorithm to estimate large phylogenies by maximum likelihood. *Syst Biol*. 52(5):696–704.
- Hanifin CT. 2010. The chemical and evolutionary ecology of tetrodotoxin (TTX) toxicity in terrestrial vertebrates. *Mar Drugs*. 8(3):577–593.
- Hanifin CT, Brodie ED Jr, Brodie ED III. 2008. Phenotypic mismatches reveal escape from arms-race coevolution. *PLoS Biol*. 6(3):471–482.
- Herzog RI, Cummins TR, Ghassemi F, Dib-Hajj SD, Waxman SG. 2003. Distinct repriming and closed-state inactivation kinetics of Na_v1.6 and Na_v1.7 sodium channels in mouse spinal sensory neurons. *J Physiol (Lond)*. 551(3):741–750.
- Hoekstra HE, Coyne JA. 2007. The locus of evolution: evo devo and the genetics of adaptation. *Evolution* 61(5):995–1016.
- Hoekstra HE, Hirschmann RJ, Bunday RA, Insel PA, Crossland JP. 2006. A single amino acid mutation contributes to adaptive beach mouse color pattern. *Science* 313(5783):101–104.
- Hong X, Scofield DG, Lynch M. 2006. Intron size, abundance, and distribution within untranslated regions of genes. *Mol Biol Evol*. 23(12):2392–2404.
- Isbister GK, Kiernan MC. 2005. Neurotoxic marine poisoning. *Lancet Neurol*. 4(4):219–228.
- Janes DE, Valenzuela N, Ezaz T, Amemiya C, Edwards SV. 2011. Sex chromosome evolution in amniotes: applications for bacterial artificial chromosome libraries. *J Biomed Biotechnol*. 2011(2011):132975.
- Jost MC, Hillis DM, Lu Y, Kyle JW, Fozzard HA, Zakon HH. 2008. Toxin-resistant sodium channels: parallel adaptive evolution across a complete gene family. *Mol Biol Evol*. 25(6):1016–1024.
- Kao CY. 1966. Tetrodotoxin, saxitoxin and their significance in the study of excitation phenomena. *Pharmacol Rev*. 18(2):997–1049.
- Kao CY, Fuhrman FA. 1963. Pharmacological studies on tarichatoxin, a potent neurotoxin. *J Pharmacol Exp Ther*. 140(1):31–40.
- Kellner WA, Sullivan RT, Carlson BH, Thomas JW, Prog NCS. 2005. Uprobe: a genome-wide universal probe resource for comparative physical mapping in vertebrates. *Genome Res*. 15(1):166–173.
- Kenny TP, Shivers RR. 1974. Blood-brain barrier in a reptile, *Anolis carolinensis*. *Tissue Cell* 6(2):319–333.
- Kent WJ. 2002. BLAT—The BLAST-like alignment tool. *Genome Res*. 12(4):656–664.
- Kiernan MC, Isbister GK, Lin CSY, Burke D, Bostock H. 2005. Acute tetrodotoxin-induced neurotoxicity after ingestion of puffer fish. *Ann Neurol*. 57(3):339–348.
- Kohany O, Gentles AJ, Hankus L, Jurka J. 2006. Annotation, submission and screening of repetitive elements in Repbase: RepbaseSubmitter and Censor. *BMC Bioinformatics* 7:474.
- Koressaar T, Remm M. 2007. Enhancements and modifications of primer design program Primer3. *Bioinformatics* 23(10):1289–1291.
- Lee CH, Jones DK, Ahern C, Sarhan MF, Ruben PC. 2011. Biophysical costs associated with tetrodotoxin resistance in the sodium channel pore of the garter snake, *Thamnophis sirtalis*. *J Comp Physiol A*. 197(1):33–43.
- Liebeskind BJ, Hillis DM, Zakon HH. 2011. Evolution of sodium channels predates the origin of nervous systems in animals. *Proc Natl Acad Sci U S A*. 108(22):9154–9159.
- Moczydlowski EG. 2013. The molecular mystique of tetrodotoxin. *Toxicol* 63:165–183.
- Onkal R, Mattis JH, Fraser SP, Diss JKJ, Shao D, Okuse K, Djamgoz MBA. 2008. Alternative splicing of Nav1.5: an electrophysiological

- comparison of “neonatal” and “adult” isoforms and critical involvement of a lysine residue. *J Cell Phys.* 216(3):716–726.
- Penzotti JL, Fozzard HA, Lipkind GM, Dudley SC. 1998. Differences in saxitoxin and tetrodotoxin binding revealed by mutagenesis of the Na⁺ channel outer vestibule. *Biophys J.* 75(6):2647–2657.
- Rockman MV. 2012. The QTN program and the alleles that matter for evolution: all that’s gold does not glitter. *Evolution* 66(1):1–17.
- Rosenberg HI. 1973. Functional anatomy of pulmonary ventilation in the garter snake, *Thamnophis elegans*. *J Morphol.* 140: 171–184.
- Rosenblum EB, Hoekstra HE, Nachman MW. 2004. Adaptive reptile color variation and the evolution of the Mc1r gene. *Evolution* 58(8):1794–1808.
- Ross MT, LaBrie SL, McPherson J, Stanton VP Jr. 1999. Screening large-insert libraries by hybridization. *Curr Protoc Hum Genet.* 21: 5.6.1–5.6.52.
- Rowe AH, Xiao YC, Rowe MP, Cummins TR, Zakon HH. 2013. Voltage-gated sodium channel in grasshopper mice defends against bark scorpion toxin. *Science* 342(6157):441–446.
- Sawyer S. 1989. Statistical tests for detecting gene conversion. *Mol Biol Evol.* 6(5):526–538.
- Schwartz TS, Tae H, Yang Y, Mockaitis K, Van Hemert JL, Proulx SR, Choi J, Bronikowski AM. 2010. A garter snake transcriptome: pyrosequencing, *de novo* assembly, and sex-specific differences. *BMC Genomics* 11:694.
- Shedlock AM. 2006. Phylogenomic investigation of CR1 LINE diversity in reptiles. *Syst Biol.* 55(6):902–911.
- Shedlock AM, Botka CW, Zhao SY, Shetty J, Zhang TT, Liu JS, Deschavanne PJ, Edwards SV. 2007. Phylogenomics of nonavian reptiles and the structure of the ancestral amniote genome. *Proc Natl Acad Sci U S A.* 104(8):2767–2772.
- Steiner CC, Weber JN, Hoekstra HE. 2007. Adaptive variation in beach mice produced by two interacting pigmentation genes. *PLOS Biol.* 5(9):1880–1889.
- Stern DL, Orgogozo V. 2008. The loci of evolution: how predictable is genetic evolution? *Evolution* 62(9):2155–2177.
- Stern DL, Orgogozo V. 2009. Is genetic evolution predictable? *Science* 323(5915):746–751.
- Terlau H, Heinemann SH, Stuhmer W, Pusch M, Conti F, Imoto K, Numa S. 1991. Mapping the site of block by tetrodotoxin and saxitoxin of sodium channel II. *FEBS Lett.* 293(1–2):93–96.
- Thornton JW, DeSalle R. 2000. Gene family evolution and homology: genomics meets phylogenetics. *Annu Rev Genomics Hum Genet.* 1: 41–73.
- Travisano M, Shaw RG. 2013. Lost in the map. *Evolution* 67(2):305–314.
- Trimmer JS, Rhodes KJ. 2004. Localization of voltage-gated ion channels in mammalian brain. *Annu Rev Phys.* 66:477–519.
- Untergasser A, Cutcutache I, Koressaar T, Ye J, Faircloth BC, Remm M, Rozen SG. 2012. Primer3-new capabilities and interfaces. *Nucleic Acids Res.* 40(15):e115.
- Vonk FJ, Casewell NR, Henkel CV, Heimberg AM, Jansen HJ, McCleary RJR, Kerckamp HME, Vos RA, Guerreiro I, Calvete JJ, et al. 2013. The king cobra genome reveals dynamic gene evolution and adaptation in the snake venom system. *Proc Natl Acad Sci U S A.* 110(51):20651–20656.
- Vornanen M, Hassinen M, Haverinen J. 2011. Tetrodotoxin sensitivity of the vertebrate cardiac Na⁺ current. *Mar Drugs.* 9(11):2409–2422.
- Widmark J, Sundstrom G, Daza DO, Larhammar D. 2011. Differential evolution of voltage-gated sodium channels in tetrapods and teleost fishes. *Mol Biol Evol.* 28(1):859–871.
- Wu MM, Ye N, Sengupta B, Zakon HH. 2013. A naturally occurring amino acid substitution in the voltage-dependent sodium channel selectivity filter affects channel gating. *J Comp Physiol A.* 199(10):829–842.
- Yoshida S. 1994. Tetrodotoxin-resistant sodium channels. *Cell Mol Neurobiol.* 14(3):227–244.
- Yotsu-Yamashita M, Mebs D. 2001. The levels of tetrodotoxin and its analogue 6-epitetrodotoxin in the red-spotted newt. *Notophthalmus viridescens*. *Toxicon* 39(8):1261–1263.
- Yu FH, Catterall WA. 2003. Overview of the voltage-gated sodium channel family. *Genome Biol.* 4(3):207.
- Yu FH, Yarov-Yarovoy V, Gutman GA, Catterall WA. 2005. Overview of molecular relationships in the voltage-gated ion channel superfamily. *Pharmacol Rev.* 57(4):387–395.
- Zakon HH. 2012. Adaptive evolution of voltage-gated sodium channels: the first 800 million years. *Proc Natl Acad Sci U S A.* 109(Suppl 1), 10619–10625.
- Zakon HH, Jost MC, Lu Y. 2011. Expansion of voltage-dependent Na⁺ channel gene family in early tetrapods coincided with the emergence of terrestriality and increased brain complexity. *Mol Biol Evol.* 28(4):1415–1424.
- Zimmer T. 2010. Effects of tetrodotoxin on the mammalian cardiovascular system. *Mar Drugs.* 8(3):741–762.
- Zimmermann K, Leffler A, Babes A, Cendan CM, Carr RW, Kobayashi J, Nau C, Wood JN, Reeh PW. 2007. Sensory neuron sodium channel Na_v1.8 is essential for pain at low temperatures. *Nature* 447(7146):855–858.